Competition between Photochemistry and Energy Transfer in Ultraviolet-Excited Diazabenzenes. 3. Photofragmentation and Collisional Quenching in Mixtures of 2-Methylpyrazine and Carbon Dioxide†

Eric T. Sevy,‡ Mark A. Muyskens,§ Zhen Lin,|| and George W. Flynn*

Department of Chemistry and Columbia Radiation Laboratory, Columbia University, New York, New York 10027

Received: February 22, 2000; In Final Form: July 17, 2000

The quantum yield for HCN formation via 248 and 266 nm photodissociation of methylpyrazine ($C_5N_2H_6$) is determined by IR diode probing. HCN is produced at two different dissociation rates, one of which is extremely prompt. The total quantum yield is $\phi = 0.93 \pm 0.08$ for 248 nm and 0.35 ± 0.05 for 266 nm excitation. Analysis of the quenching data within the context of a gas kinetic, strong collision model allows an estimate of the rate constant for HCN production via "late" methylpyrazine photodissociation, $k_{d1s} = 6.4 \times 10^4\ s^{-1}$ and $k_{d1s} = 4.9 \times 10^3\ s^{-1}$ for 248 and 266 nm excitation, respectively. The rate constant for "prompt" dissociation is too large to be measured using this technique. After 266 nm excitation methylpyrazine lives more than an order of magnitude longer than after 248 nm excitation. Methylpyrazine also lives more than twice as long as pyrazine excited under identical conditions. Transient absorption measurements probing rotationally and translationally excited CO_2 molecules produced following excitation of methylpyrazine are analyzed within the context of a kinetic scheme incorporating methylpyrazine photodissociation, as well as excitation of CO_2 by both translationally hot HCN and vibrationally excited methylpyrazine. This analysis indicates that vibrationally hot methylpyrazine, which has sufficient energy to dissociate, is the source of excitation in collisions imparting large amounts of rotational and translational energy to CO_2.

I. Introduction

It has long been understood that collisional energy transfer plays an important role in the process by which macroscopic systems undergo chemical change. Even in the simplest case of a unimolecular reaction, the rate constant reflects a complicated interplay between collisional activation and deactivation rates. Indeed, the competition between these processes, fragmentation and energy transfer, in highly excited molecules is essential to an understanding of any unimolecular reaction mechanism,[1] because at moderate gas densities, such as those found in planetary atmospheres, deactivating collisions may occur on a time scale similar to the decomposition process. Systems where competition between these two processes occurs can be modeled using the Lindemann mechanism for unimolecular reactions proposed over 75 years ago.[2]

Recently, a great deal of both experimental[3−6] and theoretical[7−11] effort has been expended in order to understand what role "supercollisions", events in which large amounts of energy are transferred in single collision encounters, play in the relaxation of highly vibrationally excited molecules. Studies of supercollisions in this laboratory have focused on the state-specific energy gain of simple bath molecules that have undergone collisions with highly vibrationally excited aromatic molecules. These aromatic molecules include pyrazine,[12−16] pyridine,[17] pyrimidine,[17] C_6F_6,[15,18] and 2-methylpyrazine.[19] The basic approach is to monitor the collisional quenching event in a quantum state resolved fashion by following the energy gain in spectroscopically tractable molecules through the use of a high-resolution infrared diode laser. These experiments can be summarized by the following equations:

$$\text{aromatic} + h\nu \rightarrow \text{aromatic}^{E'} \qquad \text{(production of excited donors)}$$

$$\text{aromatic}^{E'} + CO_2 \rightarrow \text{aromatic}^{E'-\Delta E} + CO_2\ (00^00;\ J,\ V) \qquad \text{(collisional quenching)}$$

$$CO_2\ (00^00;\ J,\ V) + h\nu\ (\sim 4.3\ \mu\text{m}) \rightarrow CO_2\ (00^01;\ J \pm 1,\ V) \qquad \text{(IR diode laser probe)}$$

The highly vibrationally excited donor molecule is produced by UV laser excitation followed by rapid radiationless internal conversion to the ground electronic state. This surface crossing occurs on a time scale that is fast compared to the mean collision time for these energy-transfer experiments ($t_{coll} \approx 4\ \mu s$).[20] The excited donor is quenched by collisions that produce rotationally and translationally excited CO_2 (00^00; J, V), where J is the rotational angular momentum quantum number and V represents the projection of the recoil velocity onto the probe laser axis. The nascent populations in each rovibrational state are determined by a transient absorption measurement of the strong ν_3 antisymmetric stretch band of CO_2 ($00^00 \rightarrow 00^01$) using a high-resolution CW IR diode laser ($\Delta\nu \approx 0.0003\ cm^{-1}$) operating at $\sim 4.3\ \mu$m, which allows for all the low-lying rovibrational states to be easily probed.[21,22] In addition to sensing the vibrational and rotational degrees of freedom, Doppler-broadened absorp-

† Part of the special issue "C. Bradley Moore Festschrift".

‡ Link Energy Foundation Edwin A. Link Doctoral Fellow. Present address: Department of Chemistry, Massachusetts Institute of Technology, Cambridge, MA 02139.

§ Permanent address: Department of Chemistry and Biochemistry, Calvin College, Grand Rapids, MI 49546.

|| Present address: Nortel Networks, 4100 Guardian Street, Simi Valley, CA 93063.

10.1021/jp0007033 CCC: $19.00
Published on Web 10/19/2000

tion line shapes can be measured, thereby providing information about the bath translational recoil velocities.

Over the past several years, the study of pyrazine photochemistry has increased tremendously,[23−25] including some studies of pyrazine dissociation after 248 nm absorption to form HCN.[26−29] In the pyrazine family of molecules, photochemistry and collisional deactivation occur on the same time scale. Energy transfer to bath molecules in such systems can arise either from collisions with an initially excited, vibrationally hot donor or from collisions with hot photofragments. A more comprehensive review of pyrazine photochemistry has been given elsewhere,[30] as well as an extensive study of pyrazine photofragmentation and its influence on energy transfer[31] where pyrazine is used as a donor.[12,14]

The work presented here is designed to elucidate more fully the competition between photochemistry and energy transfer in systems involving pyrazine and its methylated variants. The experiments are intended to (1) determine the rate constant for methylpyrazine photofragmentation after 248 and 266 nm UV excitation and (2) determine the identity of the donor for the large ΔE energy-transfer process in the methylpyrazine/CO_2 system.[19]

II. Experimental Section

The experimental technique for determining quantum yields has been described previously[28] and will be only briefly outlined here. A closed Pyrex cell contains gas-phase samples of methylpyrazine, in some cases mixed with CO_2 quencher gas. Typically, UV laser pulses from either a KrF excimer laser (Lambda Physik EMG 201, 15 ns pulse width) at 248 nm or a frequency-quadrupled Nd:YAG laser (Coherent NY81, 10 ns pulse width) at 266 nm excite the sample at a 1 Hz repetition rate. Studies have shown that pyrazine is extremely susceptible to multiphoton absorption;[30] therefore, because methylpyrazine is also likely to undergo multiphoton absorption, the UV pulse energy for all data in this paper will be noted in mJ/cm^2. A series of glass plates set at Brewster's angle is used to attenuate the intensity of the laser where necessary. The collimation of the ca. 1.5 cm diameter beam is adjusted to ensure that the UV beam emerges from the cell unattenuated by the 2.5 cm diameter cell aperture, and the beam is turned with a dichroic mirror coated to reflect 248/266 nm wavelengths into a joulemeter detector (Gentec, ED-200). Typically, the peak height from the UV signal is determined by averaging 40 laser pulses with a digital oscilloscope (LeCroy 9354A).

The amount of HCN photoproduct is measured by infrared absorption using an IR diode laser technique.[22] A CW, 3.1 μm diode laser beam (Mütek) propagates collinearly with the UV beam through the cell and passes through a monochromator (Bausch & Lomb, 0.5 m) to select a single diode laser mode. The diode laser controller (Laser Analytics) modulates the laser frequency over the entire P22 $00^00 \rightarrow 00^01$ absorption line of HCN at 1 kHz, and the central diode laser frequency is actively locked to an HCN reference spectral line. The digital oscilloscope records the amplified signal from a liquid nitrogen cooled InSb detector (Santa Barbara Research Center) placed at the exit slit of the monochromator. A dual-channel acquisition technique[14] is used to compensate for diode laser intensity fluctuations, and the result from the summed-average of 1000 sweeps across the absorption line is stored. This signal is usually acquired several minutes after the UV exposure is complete to allow for equilibration of the cell contents. In addition to correcting for short-term fluctuations in laser intensity, variations in diode laser power across the absorption line are corrected for by subtracting the IR signal obtained from an empty cell from the absorption signals obtained from a cell filled with sample.

Active locking of the diode laser frequency to an HCN absorption line is accomplished using a separate HCN reference cell.[13] The HCN IR absorption signal from the reference cell detector is input to a lock-in amplifier (Princeton Applied Research, model 117), the output of which is used as an error signal sent to the diode laser controller, thus keeping the diode laser frequency locked to the HCN absorption transition.

The experimental technique for determining the CO_2 absorption line widths has also been described in detail elsewhere.[22] The same experimental setup described above is used with three notable exceptions. First, the 3.1 μm diode laser is replaced by a lead salt diode laser operating at ~4.3 μm (Laser Analytics). Second, a flowing 1:1 gas mixture of methylpyrazine and CO_2 passes though a 3.0 m collision cell. The total gas pressure of 20 mTorr is maintained such that the 1 μs detection time is approximately one-quarter of the time required for an average gas kinetic collision. Third, a fraction (~10%) of the diode beam is sent through a Fabry-Perot Etalon and monochromator, rather than a reference cell, and detected by an additional InSb detector (Santa Barbara Research Corp.). The signal from this detector is used as a reference for a lock-in amplifier (Stanford Research Systems SR-510). This arrangement allows the diode laser frequency to be locked to the peak of a fringe from the scanning Fabry-Perot Etalon, which is then tuned across the line shape. The measurement of CO_2 absorption line shapes is accomplished by collecting transient absorption signals as a function of diode frequency at $t = 1.0$ μs after the UV laser pulse fires.

Methylpyrazine (Aldrich, 99+%) is purified by several freeze (77 K)/pump/thaw cycles and CO_2 (Matheson, 99.995%) is used without further purification. Gas pressures in the cell were monitored using a 1 Torr (MKS-Baratron 220C) capacitance manometer.

III. Results

A. Self-Quenching of Excited Methylpyrazine. The HCN quantum yield from methylpyrazine after 248 and 266 nm excitation has been measured as a function of methylpyrazine pressure. The method for calculating these yields from the raw absorption data has been given in detail elsewhere.[30] The dramatic decline in the HCN quantum yield from UV-excited methylpyrazine as a function of increasing pressure over three decades is shown in Figure 1a. The quantum yields from 266 nm excitation are significantly smaller than the 248 nm values at the same pressures. Note that the quantum yield falls to less than half of its maximum value (0.9 ± 0.15 for 248 nm and 0.32 ± 0.05 for 266 nm), found at the lowest pressure, within the first decade (1−10 mTorr). That significant quenching occurs at these low pressures suggests that the photodissociation process for methylpyrazine is quite slow, occurring on a microsecond time scale, similar to that observed for pyrazine.[28,30] Another feature of these quenching curves is that the quantum yield in the limit of high pressure appears to level off at some small nonzero value. This is the clearest evidence of HCN produced at a second, faster rate that is, therefore, less easily quenched. At higher pressures this HCN production will eventually be quenched. A careful study of this phenomenon in pyrazine indicated that this second, fast HCN product is the result of multiphoton absorption by pyrazine.[30] Methylpyrazine, with similar basic structure, is also susceptible to multiphoton absorption, which can then result in the production of "prompt" or quickly formed HCN via fragmentation of two or three photon excited parent molecules.

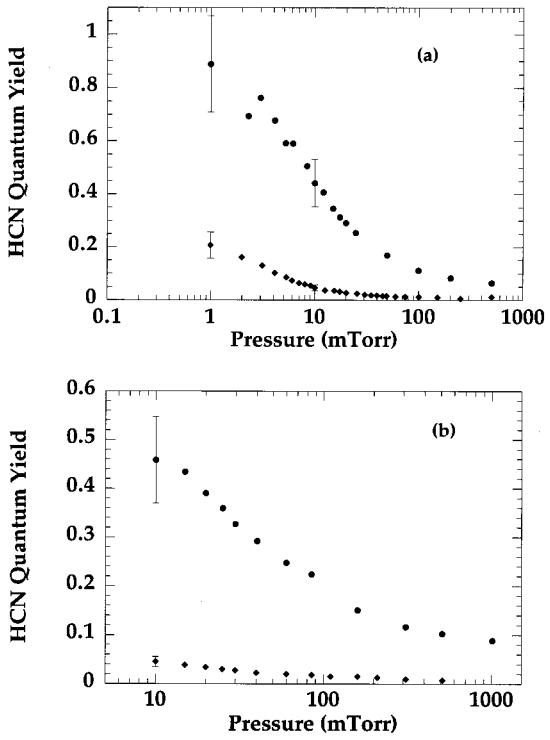

Figure 1. Quenching curves showing the dependence of the HCN quantum yield on pressure. (a) Collisional quenching of excited methylpyrazine by unexcited methylpyrazine. The circles represent the data after 248 nm excitation, and the diamonds represent the data after 266 nm excitation. (b) CO_2-quenching curves for methylpyrazine showing the dependence of the HCN quantum yield on total pressure (in a mixture of 10 mTorr of methylpyrazine with balance CO_2); the circles are for 248 nm excitation, and the diamonds are for 266 nm excitation. Quantum yield measurements obtained were conducted at a UV laser fluence of 13.9 and 4.7 mJ/cm^2 for 248 and 266 nm, respectively.

B. CO_2 Quenching of Excited Methylpyrazine. The HCN quantum yield dependence on added CO_2 acting as a quencher is displayed in Figure 1b, where the total pressure is the result of a mixture of 10 mTorr of methylpyrazine with various amounts of CO_2 (e.g., 20 mTorr total pressure with equal amounts of methylpyrazine and CO_2). The overall features of decreasing quantum yield and apparent nonzero quantum yield at high pressure seen in Figure 1a are present here as well. The quantum yield at 10 mTorr (only methylpyrazine) agrees reasonably well with corresponding data in Figure 1a; therefore, these curves clearly show the relative quenching effectiveness of CO_2 versus methylpyrazine.[32,33]

C. Energy-Transfer-Broadened Line Widths of CO_2. The translational energy of CO_2 molecules scattering into $J = 72$ following photoexcitation of methylpyrazine has been determined by measuring the nascent Doppler-broadened line shape for the absorption transition CO_2 (00^00; 72) $\rightarrow$ CO_2 (00^01; 71) at 2277.4275 cm^{-1}. These measured line shapes fit well to a Gaussian function, indicating an isotropic distribution of CO_2 velocities. The transient absorption line shapes obtained from measurements taken 1 μs after the UV laser fires on a flowing mixture of 10 mTorr of methylpyrazine and 10 mTorr of CO_2 using both 248 and 266 nm excitation are shown in Figure 2. The fitted line width (full width at half-maximum) obtained from CO_2 scattered by methylpyrazine excited to $\approx$41 000 cm^{-1} is $\Delta\nu = 0.0087 \pm 0.001$ cm^{-1}, in good agreement with previously reported values.[19] The translational temperatures of the CO_2 molecules recoiling from the excited donor are evaluated using the relationship

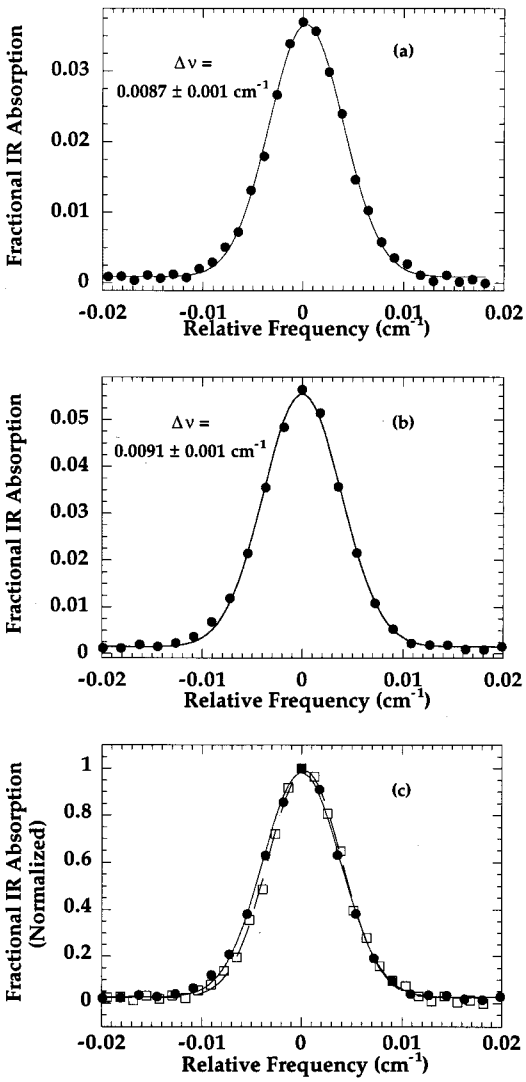

Figure 2. Doppler-broadened line shapes for the CO_2 (00^00; $J = 72$) $\rightarrow$ CO_2 (00^01; $J = 71$) infrared transition at 2277.4277 cm^{-1}. The data for a flowing 1:1 gas mixture of 10 mTorr of methylpyrazine and 10 mTorr of CO_2 are shown by the solid circles, and the solid lines represent a best nonlinear least-squares fit to a Gaussian function. Data are collected 1.0 μs following (a) 248 nm methylpyrazine excitation and (b) 266 nm methylpyrazine excitation. (c) Both line shapes are plotted together for direct comparison (the solid circles are for 266 nm excitation, while the open squares are for 248 nm excitation). The transition line widths (full width at half-maximum) obtained from the line profiles are (a) 0.0087 ± 0.001 cm^{-1} and (b) 0.0091 ± 0.001 cm^{-1}, only slightly different from each other, indicating that a large amount of translational energy is transferred to CO_2 in collisions with methylpyrazine excited to the two different energies. Line width values are summarized in Table 1.

$$T_f^{CO_2} = \frac{mc^2(\Delta\nu_{obs})^2}{8R\ \ln 2\ (\nu_o)^2} \qquad (1)$$

where m is the mass of CO_2, c is the speed of light, $\Delta\nu_{obs}$ is the fitted line shape (full width at half-maximum), R is the gas constant, and ν_o is the frequency at the center of the absorption line. From this, the center of mass translational temperature, T_f^{com}, of 1270 $\pm$ 190 K can be calculated using[14]

$$T_f^{com} = T_f^{CO2} + (T_f^{CO2} - T)\left(\frac{m_{CO_2}}{m_{Mpyr}}\right) \qquad (2)$$

where T_f^{CO2} is the temperature describing the CO_2 lab-frame

velocity distribution calculated using eq 1, T is the collision cell temperature, and the m_i are the respective masses of the collision partners.

At 266 nm excitation energy, the excited methylpyrazine molecule initially has about 3000 cm^{-1} less energy than after excitation at 248 nm; however, the fitted CO_2 line width for 266 nm excitation is nearly identical to that for 248 nm excitation, $\Delta\nu = 0.0091 \pm 0.001$ cm^{-1}, corresponding to a center-of-mass translational temperature of 1400 ± 200 K. The transient absorption line shapes for CO_2 00^00, $J = 72$, were measured at a series of 248 nm UV laser fluences ranging from 5.2 to 63.9 mJ/cm^2. The line widths ($\Delta\nu = 0.009 \pm 0.001$ cm^{-1}) over this range of laser fluence are identical within experimental error indicating that the translational energy transfer is independent of UV pump laser intensity. The line width values and translational temperatures from the Doppler-broadened line shapes are summarized in Table 1.

TABLE 1: Doppler-Broadened Line Widths ($\Delta\nu_{obs}$) and Corresponding Center-of-Mass Translational Temperatures (T_f^{com}) for CO_2 Molecules Probed 1 μs after UV-Laser Excitation of Methylpyrazine As Derived from the Fits to Transient Absorption Data

excitation wavelength (cm^{-1})	pump laser fluence (mJ/cm^2)	$\Delta\nu_{obs}$ (cm^{-1})[a]	T_f^{com} (K)[b]
266	4.7	0.0091	1400 ± 200
248	5.2	0.0090	1370 ± 200
248	10.3	0.0086	1240 ± 190
248	23.1	0.0099	1680 ± 220
248	42.7	0.0088	1300 ± 200
248	63.9	0.0095	1540 ± 210

[a] The error in the experimentally measured line widths is ± 0.001 cm^{-1}. [b] Calculated using eqs 1 and 2.

IV. Discussion

A. Photodissociation Kinetics. As with pyrazine,[28,30] the quenching data can be used to estimate the first-order rate constant for the photoproduction of HCN and hence the lifetime of the hot parent molecule. A model that includes multiphoton (prompt) dissociation and the possibility that two HCN molecules are formed in the photodissociation (either initially or sequentially) has been developed elsewhere[30] and can be used to fit the data for methylpyrazine. The following kinetic scheme describes this model and serves to define the meaning of the kinetic rate constants for each step:

$$\text{Mpyr} + h\nu \rightarrow \text{Mpyr}^{E'}; \quad \text{one-photon laser excitation} \quad (3)$$

$$\text{Mpyr}^{E'} + h\nu \rightarrow \text{Mpyr}^{2E'}; \quad \text{multiphoton laser excitation} \quad (4)$$

$$\text{Mpyr}^{2E'} + \text{Q} \xrightarrow{k_{qp}} \text{Mpyr}^{2E'-\Delta E} + \text{Q}^{\Delta E}; \quad \text{quenching of high-energy species} \quad (5)$$

$$\text{Mpyr}^{E'} + \text{Q} \xrightarrow{k_{qs}} \text{Mpyr}^{E'-\Delta E} + \text{Q}^{\Delta E}; \quad \text{quenching of low-energy species} \quad (6)$$

$$\text{Mpyr}^{2E'} \xrightarrow{k_{d1p}} \text{HCN}^* + \text{C}_4\text{H}_5\text{N}; \quad \text{“prompt” dissociation} \quad (7)$$

$$\text{Mpyr}^{2E'} \xrightarrow{k_{d1p'}} \text{CH}_3\text{CN}^* + \text{C}_3\text{H}_3\text{N}; \quad \text{prompt dissociation} \quad (8)$$

$$\text{Mpyr}^{E'} \xrightarrow{k_{d1s}} \text{HCN}^* + \text{C}_4\text{H}_5\text{N}; \quad \text{“late” dissociation} \quad (9)$$

$$\text{Mpyr}^{E'} \xrightarrow{k_{d1s'}} \text{CH}_3\text{CN}^* + \text{C}_3\text{H}_3\text{N}; \quad \text{late dissociation} \quad (10)$$

$$\text{Mpyr}^{E'} \xrightarrow{k_{d2s}} 2\text{HCN}^* + \text{HCCCH}_3; \quad \text{late dissociation} \quad (11)$$

$$\text{Mpyr}^{E'} \xrightarrow{k_{d2s'}} \text{HCN}^* + \text{CH}_3\text{CN} + \text{C}_2\text{H}_2; \quad \text{late dissociation} \quad (12)$$

The time-dependent behavior of the $Mpyr^{E'}$, the $Mpyr^{2E'}$, and the HCN species can be readily obtained from the differential equations describing the kinetic scheme, which at long times can be rearranged to give the quantum yield ϕ

$$\phi = \left(\frac{1}{\phi_m} + \frac{t_d}{t_{coll}}\right)^{-1} + \phi_u \quad (13)$$

where $t_d = 1/(k_{d1s} + 2k_{d2s} + k_{d2s'})$ f_s is the effective lifetime of the excited methylpyrazine, $\phi_m = (k_{d1s} + 2k_{d2s} + k_{d2s'})f_s/(k_{d1s} + k_{d2s} + k_{d1s'} + k_{d2s'})$ is the maximum quantum yield from “late” dissociation, and $t_{coll} = 1/k_{qs}[Q]$ is the mean hard sphere collision time. In this expression for ϕ, the last term, $\phi_u = k_{d1p} f_p/(k_{d1p} + k_{d1p'} + k_{qp}[Q])$ is associated with prompt “unquenched” dissociation. Regardless of the pressure used in the present experiments, this term is not eliminated and is, therefore, essentially constant with respect to the collision rate ($\gamma \sim k_{d1p} + k_{d1p'} \gg k_{qp}[Q]$). f_p and f_s have been defined as the fraction of methylpyrazine molecules that initially undergo multiphoton excitation and single-photon excitation, respectively. As has been discussed elsewhere, prompt dissociation in the pyrazine case can be associated with parent molecules having absorbed two photons.[30] The unimolecular rate constant associated with a species excited to 80 000 cm^{-1} is, of course, much larger than that for a species at an energy of 40 000 cm^{-1}.

Equation 13 forms the basis for a three-parameter, nonlinear least-squares fit that determines t_d, ϕ_m, and ϕ_u for each data set. Figure 3 displays the resulting fits, and Table 2 summarizes the parameters. The methylpyrazine complex lifetime after 248 nm excitation is $t_d = 16 \pm 2$ μs. Note also that the lifetime for methylpyrazine excited to 37 910 cm^{-1} is even longer than this (204 ± 8 μs), again highlighting the fact that these molecules with “chemically significant” amounts of internal energy live for a very, very long time before fragmenting.

The methylpyrazine dissociation rate derived from self-quenching studies (6.4×10^4 s^{-1}) is smaller than that derived from CO_2 quenching studies (1.8×10^5 s^{-1}) after 248 nm excitation. Similarly, for self-quenching and CO_2 quenching after 266 nm excitation, $1/t_d = 4.9 \times 10^3$ and 9.3×10^3 s^{-1}, respectively, are the values obtained for the dissociation rate. This is consistent with the earlier qualitative observation that CO_2 is less effective than unexcited methylpyrazine at quenching and is merely a limitation of applying the strong collision model equally to both quenchers. Because unexcited methylpyrazine is the most efficient strong collision partner, the dissociation rate constant from self-quenching data is then an *upper limit* for the dissociation process; the “true” dissociation rate for methylpyrazine must be even smaller than measured here. Note also that the *differences* in the lifetime between self-quenching and CO_2 quenching are smaller at 37 910 cm^{-1} than at 40 640 cm^{-1}, indicating as expected that methylpyrazine is much closer to its critical energy E_o for fragmentation to form HCN at 37 910 cm^{-1} than at 40 640 cm^{-1}.

This model also provides a reasonable basis for analyzing quantum yields below 1 ($\phi_m = 0.32$ for the 266 nm self-quenching data). For these results to make sense, there must be some “dark” channel (that does not produce HCN) available to methylpyrazine excited by 266 nm radiation. It is possible that

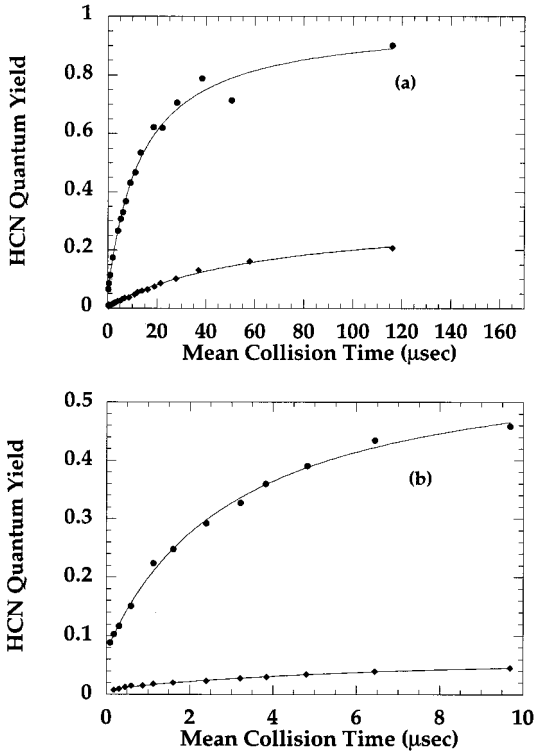

Figure 3. Quantum yield displayed as a function of the mean collision time for (a) self-quenching studies and (b) CO_2-quenching studies. (The mean collision times for the data sets have been calculated according to the equations shown in footnote a of Table 2.) Circles are for 248 nm excitation, while diamonds are for 266 nm excitation. The solid lines are the result of a three-parameter, nonlinear least-squares fit to the data using eq 13. The results of this nonlinear fit are summarized in Table 2. These data provide a value of 6.4×10^4 and 4.9×10^3 s^{-1} for the first-order photodissociation rate constant from self-quenching 248 and 266 nm studies, respectively, and 1.8×10^5 and 9.3×10^3 s^{-1} from CO_2-quenching 248 and 266 nm studies, respectively. Quantum yield measurements obtained for 248 and 266 nm excitation were conducted at a UV laser fluence of 13.9 and 4.7 mJ/cm^2, respectively.

methylpyrazine with $E_{int} = 37\,910$ cm^{-1} is so close to E_o, the energy threshold for dissociation, that the excited methylpyrazine is distributed on both sides of E_o reflecting the thermal energy spread of initially unexcited methylpyrazine. This dark HCN channel might result in the formation of other products such as acetonitrile (CH_3CN) or methylacetylene (CH_3CCH), which could account in part for the HCN quantum yields being less than one. Excitation at 266 nm, which provides the longest dissociation lifetimes (ca. 200 μs), is in the range of IR fluorescence lifetimes for highly vibrationally excited states. Thus, photodissociation at even the lowest pressures may be in competition with radiative quenching processes.[34,23,35−37] This effect has been ignored in the present analysis, as have wall collisions. Both effects will lead to $\phi_m < 1$.

The values for ϕ_m, the "maximum" quantum yield derived from the CO_2 quenching data, are smaller than those derived from the methylpyrazine quenching data (0.52 vs 0.93, respectively, at 248 nm). The hard sphere collision model used to derive eq 13 assumes that every collision carries away enough energy to deactivate the photodissociation process. Hence this model is expected to be most accurate for the case of pure methylpyrazine, which is a stronger collider than CO_2. If the deactivating rate for CO_2, used to derive the results in Table 2, is decreased below the strong collider, gas kinetic collision rate, the values for ϕ_m derived from the CO_2 data approach the results for pure methylpyrazine. A similar effect is observed for the dissociation rate constant derived from the CO_2 data, which becomes smaller and approaches the methylpyrazine value when the CO_2 quenching rate is decreased below the gas kinetic value.

TABLE 2: HCN Quantum Yields, Photodissociation Lifetimes, and Photodissociation Rate Constants for the 248 and 266 nm Photofragmentation of Methylpyrazine As Derived from Fits to the Data Shown in Figure 3 Using Eq 13[a]

quencher	excitation wavelength (nm)	ϕ_m[b]	t_d[c]	ϕ_u[d]	k_s[e]
self	248	0.93 ± 0.08	16 ± 2	0.051 ± 0.016	6.4×10^4
CO_2	248	0.52 ± 0.05	6.0 ± 0.4	0.072 ± 0.014	1.8×10^5
self	266	0.32 ± 0.05	204 ± 8	0.005 ± 0.001	4.9×10^3
CO_2	266	0.06 ± 0.01	108 ± 12	0.008 ± 0.002	9.3×10^3

[a] Data were collected at $I_{laser} = 4.7$ and 13.9 mJ/cm^2 for 266 and 248 nm studies, respectively. The fit parameters obtained from the data sets shown in Figure 3 were obtained using a hard sphere collision rate given by $k_{qs} = k_{coll} = \sqrt{(8k_BT\pi)/\mu}\{(d_Q + d_{methylpyrazine})/2\}^2$, where d_Q is the diameter of the quencher, either CO_2 ($d_{CO_2} = 4.5$ Å (ref 39)) or methylpyrazine ($d_{methylpyrazine} = 5.27$ Å (assumed to be equal to benzene, ref 39)), k_B is Boltzmann's constant, μ is the reduced mass, and T is the temperature of the collision cell. The mean collision time is then given by $t_{coll} = 1/(k_{methylpyrazine}[\text{methylpyrazine}] + k_{CO_2}[CO_2])$, where k_Q is the hard sphere rate constant above with Q as either methylpyrazine or CO_2. [b] The maximum value for the quantum yield. $\phi_m = (k_{d1s} + 2k_{d2s} + k_{d2s'})f_s/(k_{d1s} + k_{d2s} + k_{d1s'} + k_{d2s'})$; see text following eq 13 for definitions of symbols. [c] The photodissociation lifetime (i.e., the lifetime of vibrationally excited pyrazine) given in microseconds. $t_d = 1/(k_{d1s} + 2k_{d2s} + k_{d2s'})f_s$; see text following eq 13 for definitions of symbols. [d] The quantum yield for the "prompt" "unquenched" dissociation. $\phi_u \approx k_{d1p}f_p/(k_{d1p} + k_{d1p'}) \approx f_p$ see text following eq 13 for definitions of symbols. [e] The photodissociaiton rate constant given in units of s^{-1} for all the combined slow processes, $k_s = 1/t_d = (k_{d1s} + 2k_{d2s} + k_{d2s'})f_s$.

In all cases, the photodissociation lifetimes from methylpyrazine reported here are longer by about 300% than the lifetimes for pyrazine dissociation reported previously[30] (6 vs 16 μs for pyrazine and methylpyrazine 248 nm studies, respectively, and 66 vs 204 μs for pyrazine and methylpyrazine 266 nm studies, respectively). This may possibly provide some insight into the mechanism for the photofragmentation process of pyrazine.

B. Energy-Transfer Rate Analysis. Recent molecular beam studies of the photodissociation of pyrazine at 248 nm showed that of the two photofragments (HCN and C_3H_3N) only HCN possessed enough translational energy to collisionally excite a CO_2 molecule into high rotational states of the ground vibrational level.[26,27,29] On the basis of a simple prior analysis, fragments from methylpyrazine dissociation will have even less translational energy; therefore, the only fragment that could potentially compete with vibrationally excited methylpyrazine as an energy-transfer donor to CO_2 would be HCN. The analysis of the respective roles of translationally hot HCN and highly vibrationally excited methylpyrazine in producing CO_2 (00^00; $J = 72$, V) via collisions depends largely on two factors: the time dependence of the population of CO_2 (00^00; $J = 72$, V) and the amount of methylpyrazine multiphoton absorption. Using the kinetic scheme developed elsewhere,[31,30] the time-dependent behavior of the important species in the present experiments can be assessed. The results of this analysis are given below.

Prompt HCN. In the case of pyrazine as an energy-transfer donor, fluence-dependent photofragmentation studies provided a key piece of information for use in determining the dominant

donor (pyrazine vs HCN) for CO_2 scattered into $J = 72$.[30] The pyrazine fluence-dependent photofragmentation studies performed at 248 nm and the information theoretic prior function analysis of pyrazine dissociation overwhelmingly point to multiphoton absorption as the source of prompt translationally excited photoproducts, HCN*. This makes the study of the energy-transfer process as a function of UV laser fluence the most important test of energy-transfer donor identity in the case of methylpyrazine as well.

The amount of CO_2 scattered into (00^00; $J = 72$, V) per absorbed 248 nm photon, $[CO_2\ (00^00;\ J = 72,\ V)]/N_{h\nu}$, remains approximately constant when the pump laser fluence, I_{laser}, is changed by nearly a factor of 12. This change in laser fluence corresponds to a change in HCN* population produced via the multiphoton dissociation of ~145-fold. If this source of HCN* were the dominant donor for scattering CO_2 into $J = 72$ with large amounts of translational recoil, an increase in donor population would necessarily affect the scattered CO_2 populations by a factor of 145 as well. Since this is not observed, HCN* produced via prompt dissociation is clearly not the donor source in the energy-transfer process. The CO_2 recoil line widths were also found to be independent of pump laser fluence (see Table 1).

Additionally, CO_2 transient signals do not display the characteristics of energy transfer from translationally hot particles but rather the characteristics of energy transfer from vibrationally excited donors (compare Figure 1 from ref 19 to Figure 1 from ref 38). Hot, fast-moving particles produce much faster rise times for energy-transfer signals than do highly vibrationally excited molecules having a thermal (room-temperature) distribution of translational velocities. All of this is compelling evidence eliminating hot HCN* produced by prompt dissociation as the dominant energy-transfer donor.

Late HCN. The strongest feature indicating that the dominant energy-transfer donor is methylpyrazine and not late HCN* derives from the CO_2 time dependence.[31] The concentration of CO_2 arising from collisions with $Mpyr^{E'}$ increases linearly with time for small t, while the concentration of CO_2 arising from collisions with late HCN* scales as t^2. Time-resolved CO_2 IR absorption measurements for this system (see Figure 1 from ref 19) clearly show that the absorption in the ~0−4 μs regime grows linear with time indicating that vibrationally hot $Mpyr^{E'}$, not translationally hot HCN* from late dissociation, is the energy-transfer donor.

The rate of methylpyrazine dissociation at different excitation wavelengths can also be used to show that methylpyrazine, not late HCN*, is the energy-transfer donor. Before HCN* from late dissociation can become an energy-transfer donor, producing CO_2 (00^00; $J = 72$, V), it must be created. All of the late HCN* produced in the photodissociation of methylpyrazine is created on a microsecond time scale ($t_d = 16$ and 204 μs for 248 and 266 nm excitation, respectively). Because of the early energy-transfer detection time (1 μs) and the slow breakup of the methylpyrazine, the amount of hot late HCN*, which might be present in these experiments, is even smaller at 266 nm than at 248 nm; nevertheless, nearly identical recoil line widths are observed at both 248 and 266 nm for CO_2 ($J = 72$) bath molecules observed in these experiments. The similarity of the rotational and translational energy-transfer dynamics at both the 248 and 266 nm excitation wavelengths coupled with the long 266 nm dissociation lifetime (200 times longer than the probe time) argues strongly that the donor molecule in these scattering studies is vibrationally hot methylpyrazine.

V. Conclusions

The work described in this paper provides insight into the dissociation of highly vibrationally excited methylpyrazine following the absorption of UV laser radiation and the implications of that photofragmentation on recent energy-transfer studies performed using methylpyrazine as an energy-transfer donor.[19] The HCN quantum yield has been measured using high-resolution IR diode probing of the HCN photoproduct as a function of quencher gas pressure, and a hard sphere gas kinetic collision model has been employed to determine the time scale of the dissociation process (16 ± 2 and 204 ± 8 μs at 248 and 266 nm, respectively).

The energy-transfer data presented here establishes that collisions with vibrationally excited methylpyrazine scatter CO_2 molecules into high rotational states with large amounts of translational energy, rather than collisions with HCN photoproducts that are produced either promptly or later in the photodissociation process. The measured Doppler-broadened line widths for CO_2 recoil are independent of 248 nm pump laser intensity as well as pump laser frequency. A careful analysis of the data, particularly a detailed analysis of the time dependence of translationally hot HCN*, vibrationally hot methylpyrazine, and CO_2 (00^00; $J = 72$, V) eliminates hot HCN* from either prompt or late dissociation as the energy-transfer donor that creates rotationally and translationally excited carbon dioxide molecules. Rather, all data point to vibrationally hot methylpyrazine as the donor producing large ΔE "supercollisions." Further investigations of other possible photofragments (C_2H_2, CH_3CCH, and CH_3CN) are now underway to further confirm that methylpyrazine, not a photoproduct, is responsible for energy transfer in this system.

Acknowledgment. The authors thank Dr. Ralph Weston, Dr. Jack Preses, Dr. James Muckerman, Dr. Trevor Sears, and Dr. Greg Hall, and Professors Amy Mullin and Simon North for their insights and thoughts regarding this project and for many stimulating conversations. This work was performed at Columbia University and supported by the Department of Energy (DE-FG02-88ER13937). Equipment support was provided by the National Science Foundation (CHE-97-27205) and the Joint Services Electronics Program (U.S. Army, U.S. Navy, and U.S. Air Force; DAAG55-97-I-0166). E.T.S. acknowledges support from the Edwin A. Link Energy Foundation, and M.A.M. acknowledges sabbatical support from Calvin College and the Calvin College-Howard Hughes Medical Institute Grant.

References and Notes

(1) Gilbert, R. G.; Smith, S. C. *Theory of Unimolecular and Recombination Reactions*; Blackwell Scientific Publications: Oxford, UK, 1990.
(2) Lindemann, F. A. *Trans. Faraday Soc.* **1922**, *17*, 598.
(3) Hassoon, S.; Oref, I.; Steel, C. *J. Chem. Phys.* **1988**, *89*, 1743.
(4) Löhmannsröben, H. G.; Luther, K. *Chem. Phys. Lett.* **1988**, *144*, 473.
(5) Luther, K.; Reihs, K. *Ber. Bunsen-Ges. Phys. Chem.* **1988**, *92*, 442.
(6) Morgulis, J. M.; Sapers, S. S.; Steel, C.; Oref, I. *J. Chem. Phys.* **1989**, *90*, 923.
(7) Brown, N. J.; Miller, J. A. *J. Chem. Phys.* **1984**, *80*, 5568.
(8) Lendvay, G.; Schatz, G. C. *J. Phys. Chem.* **1990**, *94*, 8864.
(9) Clarke, D. L.; Thompson, K. C.; Gilbert, R. G. *Chem. Phys. Lett.* **1991**, *182*, 357.
(10) Bernshtein, V.; Oref, I. *J. Phys. Chem.* **1993**, *97*, 12811.
(11) Bollati, R. A.; Ferrero, J. C. *J. Phys. Chem.* **1994**, *98*, 3933.
(12) Mullin, A. S.; Park, J.; Chou, J. Z.; Flynn, G. W.; Weston, R. E., Jr. *Chem. Phys.* **1993**, *175*, 53.
(13) Michaels, C. A.; Mullin, A. S.; Flynn, G. W. *J. Chem. Phys.* **1995**, *102*, 6682.
(14) Mullin, A. S.; Michaels, C. A.; Flynn, G. W. *J. Chem. Phys.* **1995**, *102*, 6032.
(15) Michaels, C. A.; Flynn, G. W. *J. Chem. Phys.* **1997**, *106*, 3558.

(16) Michaels, C. A.; Mullin, A. S.; Park, J.; Chou, J. Z.; Flynn, G. W. *J. Chem. Phys.* **1998**, *108*, 2744.

(17) Sevy, E. T.; Lin, Z.; Flynn, G. W. To be published.

(18) Michaels, C. A.; Lin, Z.; Mullin, A. S.; Tapalian, H. C.; Flynn, G. W. *J. Chem. Phys.* **1996**, *106*, 7055.

(19) Sevy, E. T.; Rubin, S. M.; Lin, Z.; Flynn, G. W. *J. Chem. Phys.* **2000**, *113*, 4912.

(20) Sneh, O.; Cheshnovsky, O. *J. Chem. Phys.* **1992**, *96*, 8095.

(21) Weston, R. E., Jr.; Flynn, G. W. *Annu. Rev. Phys. Chem.* **1992**, *43*, 559.

(22) Flynn, G. W.; Weston, R. E., Jr. *J. Phys. Chem.* **1993**, *97*, 8116.

(23) Yamazaki, I.; Murao, T.; Yamanaka, T.; Yoshisara, K. *Faraday Discuss. Chem. Soc.* **1983**, *75*, 395.

(24) Doughty, A.; Mackie, J. C.; Palmer, J. M. *Twenty-Fifth Symposium (International) on Combustion;* The Combustion Institute, Pittsburgh, PA, 1994.

(25) Kiefer, J. H.; Zhang, Q.; Kern, R. D.; Yao, J.; Jursic, B. *J. Phys. Chem. A* **1997**, *101*, 7061.

(26) Chesko, J. D.; Stranges, D.; Suits, A. G.; Lee, Y. T. *J. Chem. Phys.* **1995**, *103*, 6290.

(27) Chesko, J. D. M. Ph.D. Dissertation, University of California, Berkeley, 1995.

(28) Michaels, C. A.; Tapalian, H. C.; Lin, Z.; Sevy, E. T.; Flynn, G. W. *Faraday Discuss.* **1995**, *102*, 405.

(29) Chesko, J. D.; Lee, Y. T. In *Highly Excited Molecules: Relaxation, Reaction, and Structure*; Mullin, A. S., Schatz, G. C., Eds.; American Chemical Society: Washington DC, 1997.

(30) Sevy, E. T.; Muyskens, M. A.; Rubin, S. M.; Flynn, G. W.; Muckerman, J. T. *J. Chem. Phys.* **2000**, *112*, 5829.

(31) Sevy, E. T.; Michaels, C. A.; Tapalian, H. C.; Flynn, G. W. *J. Chem. Phys.* **2000**, *112*, 5844.

(32) Hippler, H.; Troe, J. In *Bimolecular Collisions*; Ashfold, M. N. R., Baggott, J. E., Eds.; Royal Society of Chemistry: London, 1989.

(33) Barker, J. R.; Toselli, B. M. *Int. Rev. Phys. Chem.* **1993**, *12*, 305.

(34) McDonald, D. B.; Rice, S. A. *J. Chem. Phys.* **1981**, *74*, 4907.

(35) Bevilacqua, T. J.; Andrews, B. K.; Stout, J. E.; Weisman, R. B. *J. Chem. Phys.* **1990**, *92*, 4627.

(36) Bevilacqua, T. J.; Weisman, R. B. *J. Chem. Phys.* **1993**, *98*, 6316.

(37) Barker, J. R.; Brenner, J. D.; Toselli, B. M. In *Advances in Chemical Kinetics and Dynamics: Vibrational Energy Transfer Involving Large and Small Molecules*; Barker, J. R., Ed.; JAI Press Inc.: Greenwich, CT, 1995; Vol. 2B.

(38) Khan, F. A.; Kreutz, T. G.; Flynn, G. W.; Weston, R. E., Jr. *J. Chem. Phys.* **1990**, *92*, 4876.

(39) Hirschfelder, J. O.; Curtiss, C. F.; Bird, R. B. *Molecular Theory of Gases and Liquids*; John Wiley & Sons: New York, 1954.